Supporting Information

Anaerobic self-assembly of regenerable bacteria-quantum dots hybrid for solar hydrogen production

Xue-Meng Wang,[†a,b] Lin Chen,[†a,b] Ru-Li He,[a,b] Shuo Cui,[a,b] Jie Li,[a,b] Xian-Zhong Fu,[a,b] Qi-Zhong Wu,[d,b] Hou-Qi Liu,[b] Tian-Yin Huang,[c] Wen-Wei Li*[a,b]

[a]Department of Environmental Science and Engineering, University of Science & Technology of China, Hefei 230026, China

[b]USTC-CityU Joint Advanced Research Center, Suzhou Institute for Advance Research of USTC, Suzhou, 215123, China

[c]National and Local Joint Engineering Laboratory for Municipal Sewage Resource Utilization Technology, Suzhou University of Science and Technology, Suzhou, 215009, China

[d]School of Life Sciences and Medical Center, University of Science & Technology of China, Hefei 230026, China

*Corresponding author: Wen-Wei Li (wwli@ustc.edu.cn)

Experimental section

Methods for Calculating the Apparent Auantum Efficiency: The apparent quantum efficiency (AQE) of self-assembled bio-hybrid was calculated by the following formula:

$$\mathrm{AQE} = \frac{2 \times the\ number\ of\ evolved\ H_2\ molecule}{the\ number\ of\ incident\ photo} = \frac{\frac{2 \times M_{H_2} \times N_A}{W \times A \times t \times \lambda}}{\frac{hc}{}} \times 100\%$$

where N_A, n_{H2}, W, A, t, λ, h and c represent the Avogadro's constant, H_2 amount (mol), power of the Xenon lamp at a certain wavelength (W m^{-2}), active area (cm^{-2}), reaction time (h), incident light wavelength (nm), Planck constant (J•s) and speed of light (m s^{-1}), respectively.

Results and discussion

Optimization for self-assembly of bio-QDs in *E.Coli*

The precursor concentrations and bacterial density for the bio-QDs synthesis were optimized. The fluorescence intensities of bio-QDs synthesized at different precursor concentrations were measured, and the fastest rate of bio-QDs assembly was obtained at 1mM Na_2SeO_3 and 3 mM $CdCl_2$ (Fig. S4). At bacterial optical density of 2.0, bio-QDs was formed efficiently within 40 min (Fig. S5). Therefore, these optimal conditions were chosen for subsequent experiments.

Table S1. Synthesis rates and optical properties of bio-QDs reported in literature and in this study.

Organism	Material	Optical properties	Cell growth condition	Se-exposure condition	Biosynthetic condition	Ref.
Engineered *E. coli*	CdS	QY:0.007 %	-	1 h/37 ºC	3 h/37 ºC	[1]
Stenotrophomonas maltophilia	CdS	QY:0.3-2.08%	12 h/37 ºC	2 h/37 ºC	5h/37 ºC-yellow	[2]
Engineered *E. coli*	CdTe	-	-	-	24 h 37 ºC	[3]
E. coli1	CdSe	-	10-14 h/37 ºC	2 h/37 ºC	32 h/37 ºC - yellow	[4]
S. cerevisiae	CdSe	-	24 h/30 ºC	24 h/30 ºC	24 h/30 ºC - yellow	[5]
Engineered *S. cerevisiae*	CdSe	QY: 4.7%	24 h /30 ºC	24 h/30 ºC	24 / 30 ºC	[6]
Helminthosporum solani	CdSe	QY: 1 %	96 h/37 ºC	-	96 h /37 ºC	[7]
Earthworm	CdTe	QY: 8.3% Lifetime: 4.54 ns	-	-	11 days/20 ºC	[8]
Biomimetic synthesis	CdS	QY:15.8% (green), 14.1% (red)	-	-	Within days (37 ºC); Within hours (80 ºC)	[9]
E. coli	CdS_xSe_{1-x}	QY: 7.3% Lifetime: 133 ns	10 h/37 ºC	5 min/37 ºC	3.5 h/37 ºC - yellow	[10]
E. coli	**CdS_xSe_{1-x}**	**QY: 9.4% Lifetime: 90.7 ns**	**12 h/37 ºC**	**None**	**40 min/37 ºC-yellow**	**This work**

Table S2. Emission lifetime measurements of freshly isolated bio-QDs. Each curve was fitted with a three components exponential-decay function. τi are the lifetimes of each decay component and Ai their respective fractional intensity. χ^2 is the reduced chi-squared statistic. Average lifetimes were calculated based on equation: $\tau=\sum Ai\times\tau i^{2} / \sum Ai\times\tau i$.

Samples	**τ_1 (ns)**	**τ_2 (ns)**	**τ_3 (ns)**	**A1 (%)**	**A2 (%)**	**A3 (%)**	**Average lifetime (ns)**	**χ^2**
Ox-5 min	3.62±0.17	0.39±0.03	0.39±0.02	75±0.03	12±0.02	13±0.04	3.51	1.8
Ox-40 min	2.95±0.18	0.38±0.03	0.38±0.05	55±0.01	23±0.04	22±0.05	2.68	1.4
An-5 min	40.70±0.34	6.02±0.09	0.41±0.05	62±0.01	13±0.07	12±0.01	39.58	2.3
An-40 min	90.67±0.45	6.50±0.12	0.48±0.04	69±0.06	15±0.03	16±0.04	87.96	2.1

Table S3. Elemental analysis of the anaerobically-synthesized bio-QDs.

Elements	Line type	wt%	Atomic%
Se	L	34.26	32.24
Cd	L	51.52	34.06
S	K	5.34	12.38
P	K	8.89	21.32

Table S4. Primer sequences for quantitative RT-PCR.

Gene	Direction	Primer
grxA	Forward	5’-AAATTGAGCAATGAACGC-3’
	Reverse	5’-TTTCTACGGGTTTACCTG-3’
btuE	Forward	5’-TTAACGCCGCAATATGAGC-3’
	Reverse	5’-TTAATCTCTTCATCGCTGCC-3’
sodA	Forward	5’-ACCTACGTAAACAACGCCAA-3’
	Reverse	5’-ACGGTTTTCTTGTCTGCT-3’
zwf	Forward	5’-AACCTGCAAATCACCAAGC-3’
	Reverse	5’-ACGTACAAACAGTGCCTGA-3’
soxR	Forward	5’-ATTACCAGTATCCGTAACAGC-3’
	Reverse	5’-AAACGCTTCACCAATGGTC-3’

Table S5. Apparent quantum efficiency of *E. coli*-CdS_xSe_{1-x} hybrid compared with others inorganic-bio hybrids for hydrogen production in the literature.

Inorganic-bio hybrid	Material sites	Wavelength (nm)	AQE (%)	Mediator	Ref.
D. desulfuricans-CdS	Extracellular	445	23	MV	[11]
E.coli@I-HTCC	Extracellular	700	9.11	/	[12]
E.coli@TiO2	Extracellular	300	26.4	MV	[13]
E.coli@TiO2	Extracellular	300	1.57	MV	[14]
E.coli- CdS	Extracellular	620	9.59	/	[15]
E.coli-$AgInS_2/In_2S_3$	Extracellular	720	3.3	/	[16]
E.coli- CdS_xSe_{1-x}	Intracellular	420	27.56	/	[17]
S.oneidensis-$CuInS_2$ /ZnS	Periplasm	475	15.02	/	[18]
***E.coli*- CdSe**	**Intracellular**	**420**	**28.7**	**/**	**This work**

Table S6. Parameters of different water samples used for solar hydrogen production.

Wastewater type	TOC (g/L)	IC (mg/L)	TC (g/L)	pH
Aquaculture wastewater	1.52	78.64	1.60	7.93
Sewage	0.60	34.31	0.63	7.86

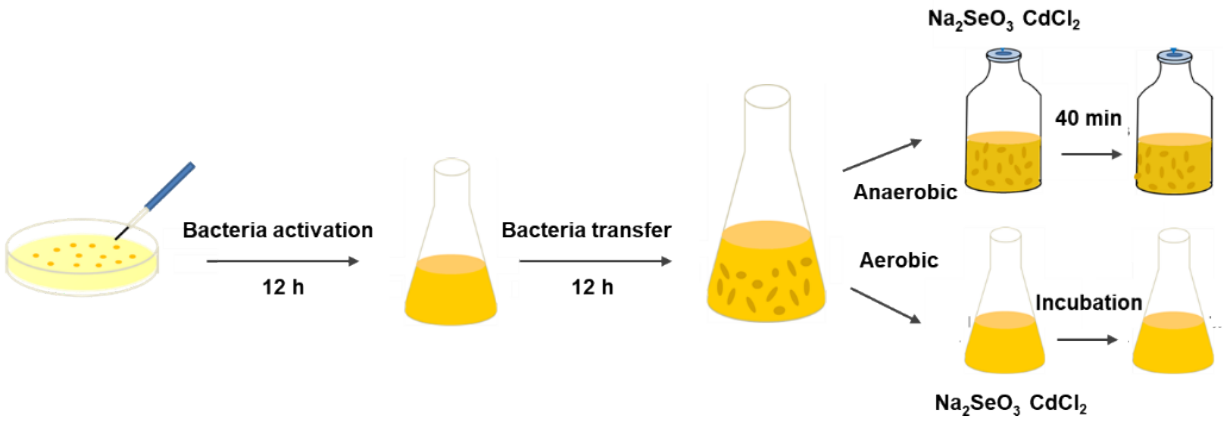

Fig. S1. Diagram of the experimental procedures for the bio-QDs synthesis.

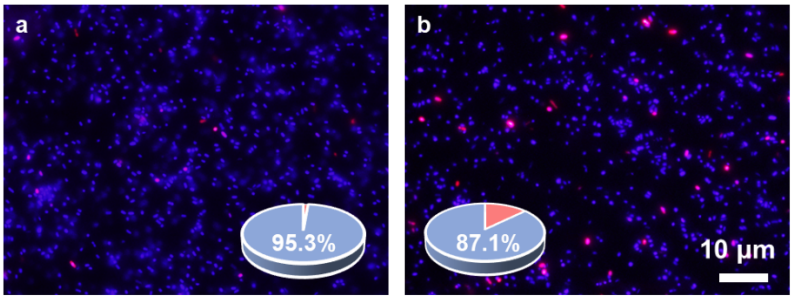

Fig. S2. Fluorescence images showing the cell viabilities after 4-h exposure to Se and Cd under (a) anaerobic and (b) aerobic incubation. The blue signals represent the alive cells and the purple red signals represent the dead cells.

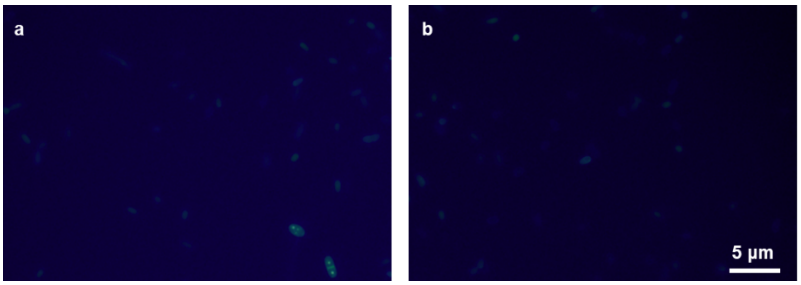

Fig. S3. Fluorescence microscopic images of *E. coli* cells co-incubated with 0.5 mM glutathione synthesis inhibitor (a) and buthionine sulfoximine (BSO); with (b) 50 µM NADPH synthesis inhibitor diphenylene iodonium.

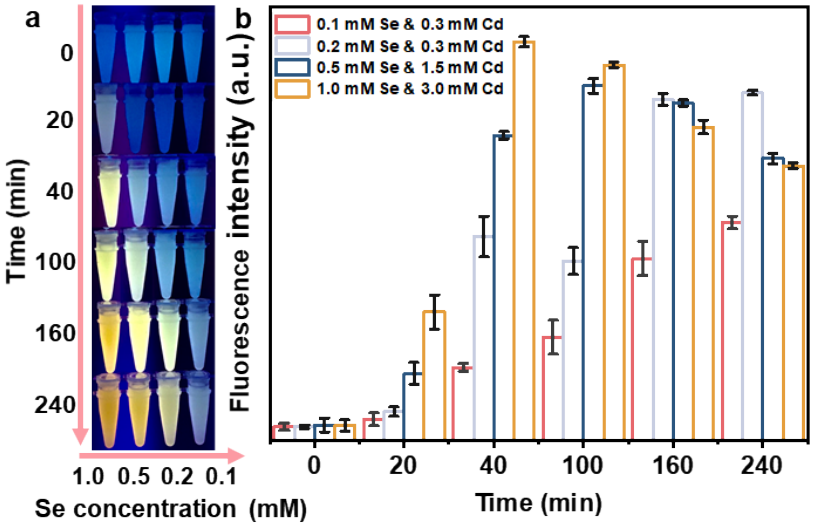

Fig. S4. Optical properties of *E. coli* cells anaerobically incubated under different precursor concentrations. (a) Images showing the fluorescence emitted by the cells in Tris-HCl buffer (pH=7.6) under UV irradiation. (b) Fluorescence intensities at 560 nm emission wavelength of cells during biosynthesis (recorded at 291 nm excitation wavelength).

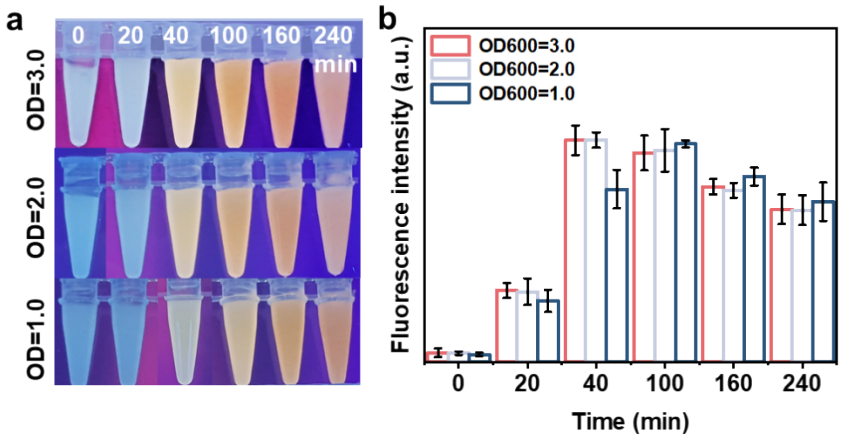

Fig. S5. Optical properties of self-assembled bio-QDs with different OD values under anaerobic condition. (a) Images showing the fluorescence emitted by the cells in Tris-HCl buffer (pH=7.6) under UV irradiation. (b) Fluorescence intensities at 430 nm emission wavelength of cells during biosynthesis (recorded at 348 nm excitation wavelengths).

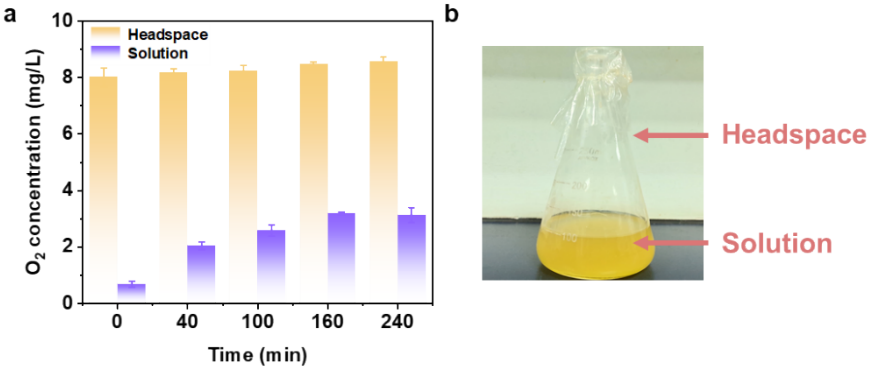

Fig. S6. (a) Oxygen concentration in conical flask headspace and solution and (b) photo of 250 mL conical flask for bio-QDs synthesis under aerobic condition.

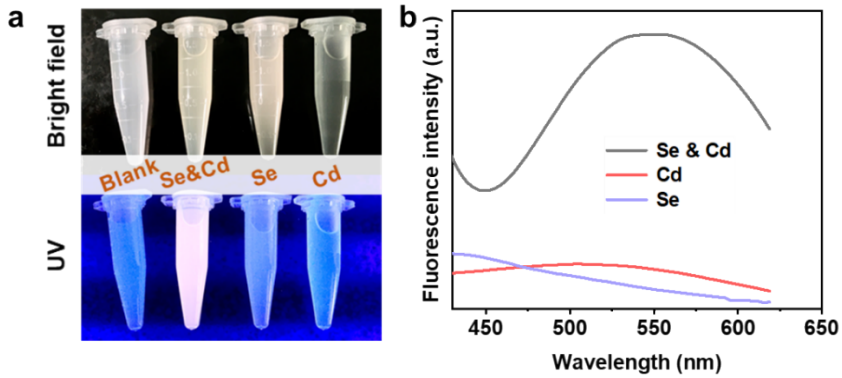

Fig. S7. (a) Optical and fluorescence images of *E. coli* cells after exposure to Se and/ or Cd under anaerobic condition. (b) Fluorescence spectra of the cells under 291-nm excitation wavelength.

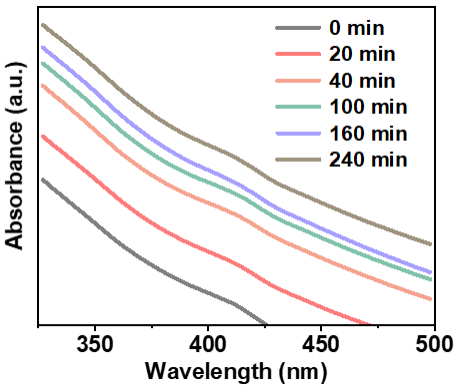

Fig. S8. Evolution of UV-vis spectra of the cells during bio-QDs synthesis under anaerobic condition.

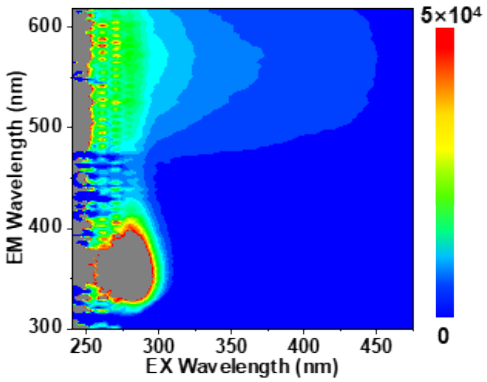

Fig. S9. Fluorescence EEM spectrum of the bio-QDs and cells under anaerobic incubation.

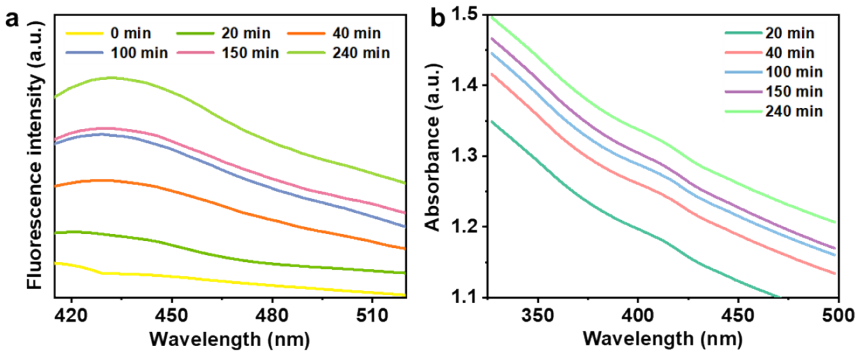

Fig. S10. Optical property changes of the cells during bio-QDs synthesis under aerobic condition: (a) Fluorescence emission spectra at 430 nm and (b) UV-vis absorption spectra.

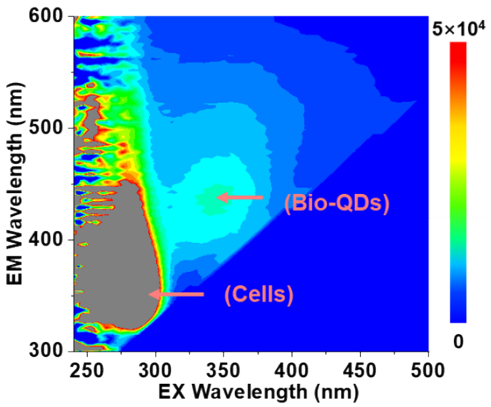

Fig. S11. Fluorescence EEM spectrum of the bio-QDs and cells under aerobic incubation.

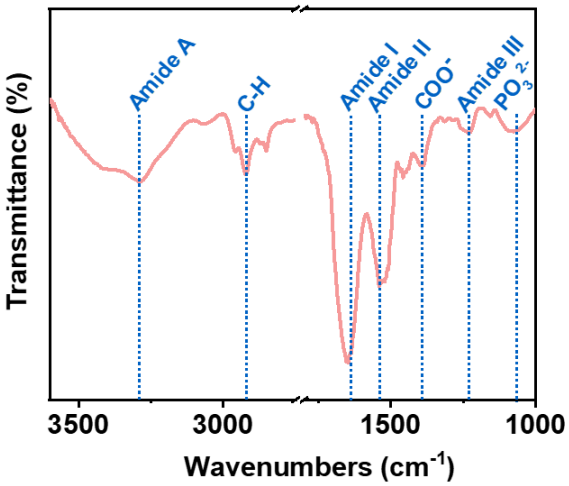

Fig. S12. FTIR spectrum of the cells with aerobically-synthesized bio-QDs.

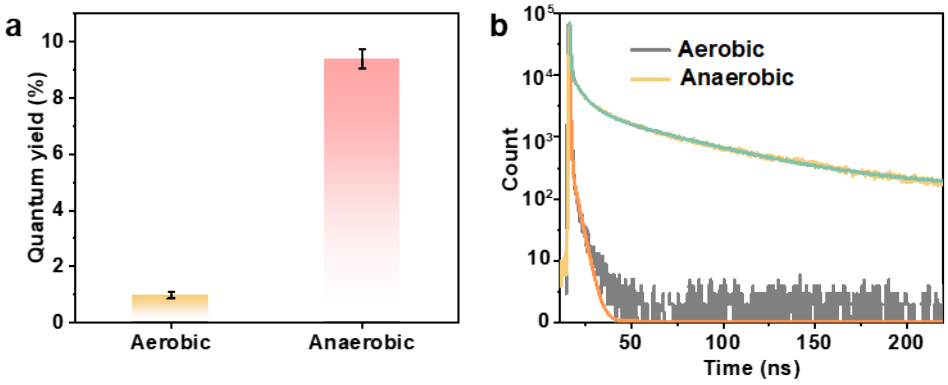

Fig. S13. Optical properties of bio-QDs synthesized from 1 Mm Na_2SeO_3 and 3 Mm $CdCl_2$. (a) Quantum yield and (b) fluorescence lifetime of the purified products after 40-min biosynthesis.

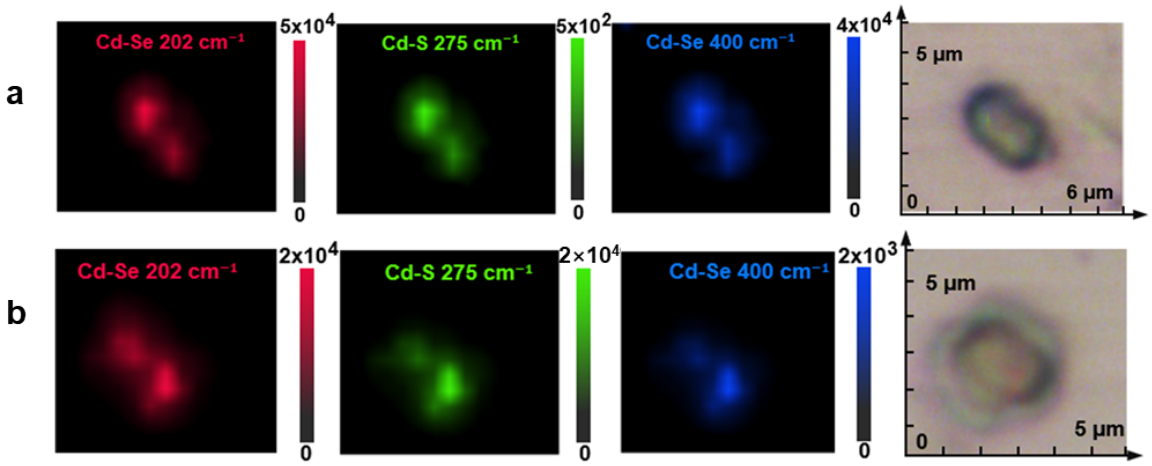

Fig. S14. Single cell Raman mapping of the bio-hybrid showing Cd-Se (at 202 cm^{-1}), Cd-S (at 275 cm^{-1}) and Se-Cd (at 400 cm^{-1}) distribution. The samples were collected after (a) 40-min anaerobic incubation and (b) 24-h aerobic incubation.

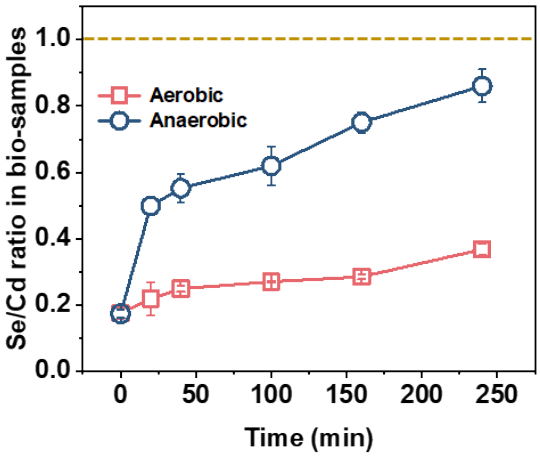

Fig. S15. Change of Se/Cd molar ratio of the biosamples during biosynthesis.

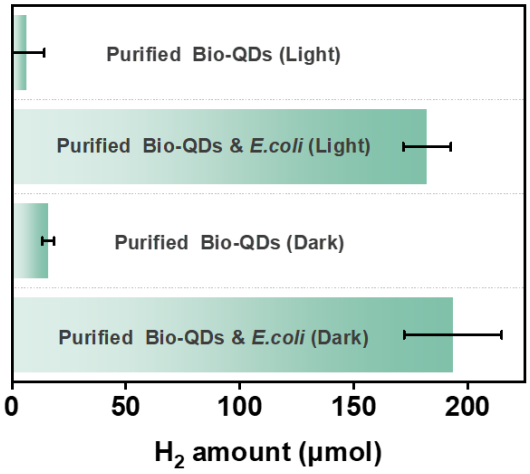

Fig. S16. Hydrogen production amount in different test groups after 3-h continuous irradiation or in the dark.

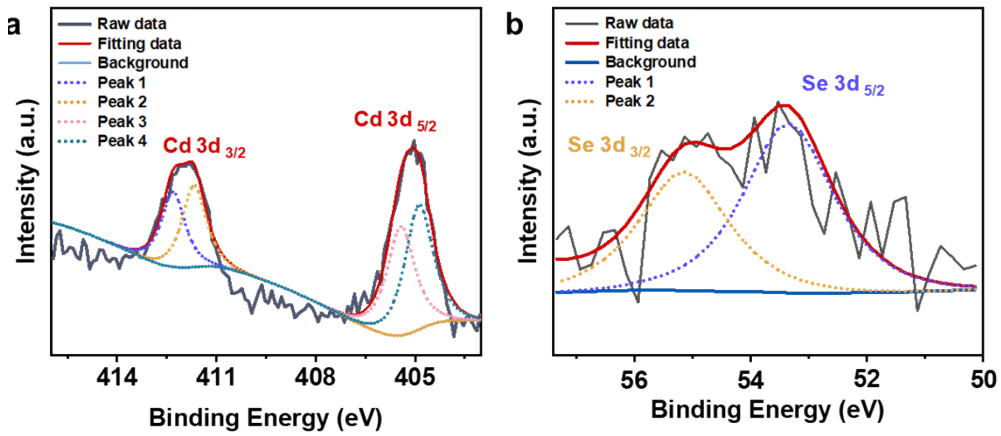

Fig. S17. XPS spectrum at the (a) Cd 3d and (b)Se 3d regions of CdSe QD after photocatalytic hydrogen production.

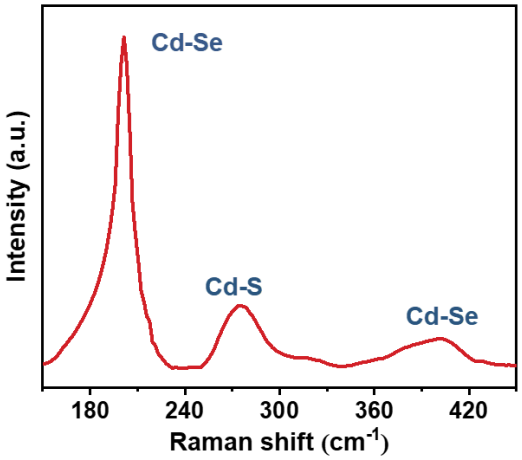

Fig. S18. In-situ Raman spectrum of the cells (under 532-nm laser irradiation) after photocatalytic hydrogen production.

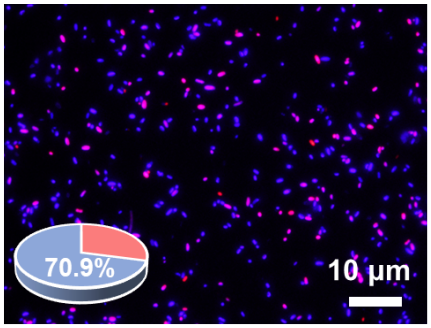

Fig. S19. Fluorescence image showing the cell viabilities after five cycles of hydrogen production tests. The blue signals represent the alive cells and the purple red signals represent the dead cells.

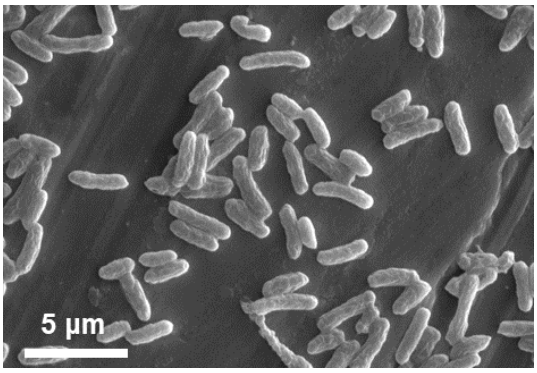

Fig. S20. SEM image of cells after refreshing the reaction medium.

Reference

1. S. H. Kang, K. N. Bozhilov, N. V. Myung, A. Mulchandani and W. Chen, *Angew. Chem. Int. Ed.*, 2008, ***47***, 5186-5189.
2. Z. Yang, L. Lu, V. F. Berard, Q. He, C. J. Kiely, B. W. Berger and S. McIntosh, *Green Chem.*, 2015, ***17***, 3775-3782.
3. V. Bansal, J. P. Monrás, V. Díaz, D. Bravo, R. A. Montes, T. G. Chasteen, I. O. Osorio-Román, C. C. Vásquez and J. M. Pérez-Donoso, *PLoS One*, 2012, *7*, e48657.
4. Z. Yan, J. Qian, Y. Gu, Y. Su, X. Ai and S. Wu, *Mater. Res. Express.*, 2014, ***1***, 015401.
5. R. Cui, H.-H. Liu, H.-Y. Xie, Z.-L. Zhang, Y.-R. Yang, D.-W. Pang, Z.-X. Xie, B.-B. Chen, B. Hu and P. Shen, *Adv. Funct. Mater.*, 2009, ***19***, 2359-2364.
6. Y. Li, Ran Cui, P. Zhang, B.-B. Chen, Z.-Q. Tian, L. Li, B. Hu, Dai-Wen Pang and Z.-X. Xie, *ACS Nano*, 2013, *7*, 2240-2248.
7. A. K. Suresh, *Spectrochim. Acta. A*, 2014, ***130***, 344-349.
8. S. R. Stürzenbaum, M. Höckner, A. Panneerselvam, J. Levitt, J. S. Bouillard, S. Taniguchi, L. A. Dailey, R. A. Khanbeigi, E. V. Rosca, M. Thanou, K. Suhling, A. V. Zayats and M. Green, *Nat. Nanotechnol.*, 2012, ***8***, 57-60.
9. R. Dunleavy, L. Lu, C. J. Kiely, S. McIntosh and B. W. Berger, *Proc. Natl. Acad. Sci. U. S. A.*, 2016, ***113***, 5275-5280.
10. L.-J. Tian, W.-W. Li, T.-T. Zhu, G.-H. Zhao, X.-W. Liu, J.-C. Dong, P.-F. An, J.-Y. Ma, F. Shen, C. Qian, B. Hu and H.-Q. Yu, *J. Mater. Chem. A*, 2019, *7*, 18480-18487.
11. M. Martins, C. Toste and I. A. C. Pereira, *Angew. Chem. Int. Ed.*, 2021, ***60***, 9055-9062.
12. K. Xiao, T. H. Tsang, D. Sun, J. Liang, H. Zhao, Z. Jiang, B. Wang, J. C. Yu and P. K. Wong, *Adv. Energy Mater.* , 2021, ***11***, 2100291.
13. Y. Honda, M. Watanabe, H. Hagiwara, S. Ida and T. Ishihara, *Appl. Catal. B Environ.*, 2017, ***210***, 400-406.
14. Y. Honda, H. Hagiwara, S. Ida and T. Ishihara, *Angew. Chem. Int. Ed.*, 2016, ***55***, 8045-8048.
15. B. Wang, C. Zeng, K. H. Chu, D. Wu, H. Y. Yip, L. Ye and P. K. Wong, *Adv. Energy Mater.* , 2017, *7*, 1700611.
16. Z. Jiang, B. Wang, J. C. Yu, J. Wang, T. An, H. Zhao, H. Li, S. Yuan and P. K. Wong, *Nano Energy*, 2018, ***46***, 234-240.
17. S. Cui, L.-J. Tian, J. Li, X.-M. Wang, H.-Q. Liu, X.-Z. Fu, R.-L. He, P. K. S. Lam, T.-Y. Huang and W.-W. Li, *Chem. Eng. J.*, 2022, ***428***, 131254.
18. B. Luo, Y. Z. Wang, D. Li, H. Shen, L. X. Xu, Z. Fang, Z. Xia, J. Ren, W. Shi and Y. C. Yong, *Adv. Energy Mater.* , 2021, ***11***, 2100256.